acta physica slovaca vol. 50 No. 4, 507 – 518 **August 2000**

PAIR–ATOMIC EFFECTS IN THE MICROMASER*

G. Ariunbold[ab1], **J. Peřina**[ac2], **Ts. Gantsog**[b3]
(a) *Department of Optics, Palacký University, 17. listopadu 50, 772 07 Olomouc, Czech Republic*
(b) *Department of Theoretical Physics of National University of Mongolia, 210646 Ulaanbaatar, Mongolia*
(c) *Joint Laboratory of Optics of Palacký University and Physical Institute of Academy of Sciences of Czech Republic, 17. listopadu 50, 772 07 Olomouc, Czech Republic*

Received 12 May 2000, accepted 12 June 2000

An average Hamiltonian, which contains pair–atomic effects, is used to develop a theory of the micromaser. A modified master equation is derived and both a steady–state and a time–dependent solutions are found showing that the trapping conditions are disturbed by influence of two–atomic events. An approximate as well as an exact spectrum are calculated and narrowing of linewidth is demonstrated within the framework of presented theory.

PACS: 42.52.+x, 42.50Dv

1 Introduction

Maser action has been achieved with, on average, less than a single excited atom in a superconducting microwave cavity [1]. Rydberg atoms, i.e., atoms having extremely large dipole moments for transitions to neighbouring levels, have been used in this one–atom maser or micromaser. Owing to very high quality factors Q achieved in the cavity, the photon lifetime was much longer than the flight time of the atom in the maser cavity [2]. A Fizeau–type velocity selector [3] can then be used in accordance with the preselection of the atomic beam velocity. Since the atomic flight time can be almost fixed, one can say that the micromaser fulfills, in an almost perfect way, the idealized conditions of Jaynes–Cummings interactions. Under this circumstance, the field produced in the cavity shows nonclassical properties [4], i.e., the number distribution of the photons in the cavity can be sub–Poissonian [5]; even a number state [6] or quantum states [7] can be generated using a cavity with a high enough quality factor. One of the very intriguing features of the micromaser is the possibility of obtaining the so–called trapping

*Presented at 7th Central-European Workshop on Quantum Optics, Balatonfüred, Hungary, April 28 – May 1, 2000.

[1]E-mail address: ariunbold@sloup.upol.cz and g_ariunbold_o@yahoo.com
[2]E-mail address: perina@risc.upol.cz
[3]E-mail address: gantsog@magicnet.mn

states. They are a direct consequence of the quantization of the electromagnetic field and just recently, they have been found experimentally [2], where the maser was pumped with a low atomic flux. Although, experimental schemes with only excited atoms show that if the field reduced density matrix is initially diagonal, it remains diagonal and studies of phase diffusion show how to create off–diagonal density matrix elements by preselecting a phase of atoms injected into the cavity [8]. The spectrum of the micromaser originating from the presence of off-diagonal matrix elements has been investigated [9]- [12]. A theory of the two–photon micromaser [13] has been developed and experiments have been carried out [14]. The linewidth of a two–photon micromaser has also been investigated [15]. However, for higher pump rates, the probability of two atom events will be non–zero [2, 16] in the micromaser cavity, because we could not strictly control the time interval between the arrival of two atoms. However, besides the usual one–photon transition, the presence of a second atom can cause two–photon transitions [17]. Co–operative atomic interactions in a single–mode laser [18] or two–atom laser [19] have been examined, too.

In the present paper, we focus ourselves on the presence of the successive pair atomic effects in the micromaser cavity and study how quantum co–operative effects can modify the standard one–atomic operation. To do this, we adopt an average Hamiltonian which can approximately describe the co–operative interactions in the micromaser. Based on derived master equations, we find the steady–state solution and spectrum of the micromaser radiation.

2 Master equations

We concentrate on a little influence of the second atom on the first one, similarly, as was considered in previous two works by Orszag et al. [16] and by Wehner et al. [17]. In standard micromaser experiments the collective events, in which two or more atoms are inside the resonator at one time, are very rare. Although, whenever two atoms are present in a microwave cavity, one can model the system by a Hamiltonian in the interaction picture and in the dipole and rotating–wave approximations as follows [18, 19]

$$\hat{H} = \hbar(g_1\hat{a}\hat{\sigma}_1^\dagger + g_1^*\hat{a}^\dagger\hat{\sigma}_1) \otimes \hat{1}_2 + \hbar(g_2\hat{a}\hat{\sigma}_2^\dagger + g_2^*\hat{a}^\dagger\hat{\sigma}_2) \otimes \hat{1}_1, \tag{1}$$

where σ_i represent the Pauli matrices for atom number i ($i = 1, 2$) and they satisfy an identity $\hat{1}_i = |a\rangle_{ii}\langle a| + |b\rangle_{ii}\langle b|$, if the upper and lower levels of the i-th atom are denoted by $|a\rangle_i$ and $|b\rangle_i$. The coefficient g_1 is an atom–field coupling constant and g_2 stands for $|g_2| = \Delta|g_1|$, where $\Delta \ll 1$, in general, they can be complex. In fact, for one atomic event we have to change the system Hamiltonian by a standard Jaynes–Cummings model, where $\Delta = 0$. More realistically, the Hamiltonian should be time–dependent, so that, Δ could be expressed, for instance, using the usual step function depending upon the time intervals that two atoms are in the cavity. The use of the step function in the Hamiltonian has been adopted by Scully et al. for the problem of a simple Langevin treatment of the laser linewidth including atomic memory effects [20]. This treatment assumes that two–atomic events are very rare. In this spirit, we can correct this calculation by adding a small term to the standard Jaynes–Cummings Hamiltonian, assuming that it is a constant, i.e., Δ =constant. This coefficient can be estimated only numerically. The use of this average Hamiltonian (1) enables us to see the qualitative characteristics due to the two atomic events. The system may be described by means of the basis $|a\rangle_1|a\rangle_2$, $|a\rangle_1|b\rangle_2$, $|b\rangle_1|a\rangle_2$

and $|b\rangle_1|b\rangle_2$, therefore, the Hamiltonian can be written as

$$\hat{H} = \begin{pmatrix} 0 & g_2\hat{a} & g_1\hat{a} & 0 \\ g_2^*\hat{a}^\dagger & 0 & 0 & g_1\hat{a} \\ g_1^*\hat{a}^\dagger & 0 & 0 & g_2\hat{a} \\ 0 & g_1^*\hat{a}^\dagger & g_2^*\hat{a}^\dagger & 0 \end{pmatrix}. \tag{2}$$

The equation of motion for the wave function $|\Psi\rangle$ for the atom–field system is

$$\frac{d}{dt}|\Psi(t)\rangle = -\frac{i}{\hbar}\hat{H}|\Psi(t)\rangle. \tag{3}$$

At any time t, the state vector $|\Psi(t)\rangle$ is a linear combination of the states $|\alpha,\beta,n\rangle$ in which the first (second) atom is in the state $|\alpha\rangle$ ($|\beta\rangle$) and the field has n photons with the probability amplitude, say, $C_{\alpha\beta n}$, therefore, it reads

$$\begin{aligned} |\Psi(t)\rangle &= \sum_n (C_{aan}(t)|a,a,n\rangle + C_{abn}(t)|a,b,n\rangle \\ &+ C_{ban}(t)|b,a,n\rangle + C_{bbn}(t)|b,b,n\rangle). \end{aligned} \tag{4}$$

The interaction energy (1) can cause transitions between the states $|a,a,n\rangle$, $|b,a,n+1\rangle$, $|a,b,n+1\rangle$ and $|b,b,n+2\rangle$. Therefore Eq. (3) becomes

$$\frac{d}{dt}\mathbf{C}(t) = -i\mathbf{M}\,\mathbf{C}(t), \tag{5}$$

where

$$\mathbf{C}(t) = \begin{pmatrix} C_{aan}(t) \\ C_{abn+1}(t) \\ C_{ban+1}(t) \\ C_{bbn+2}(t) \end{pmatrix}, \tag{6}$$

$$\mathbf{M} = \begin{pmatrix} 0 & g_2\sqrt{n+1} & g_1\sqrt{n+1} & 0 \\ g_2^*\sqrt{n+1} & 0 & 0 & g_1\sqrt{n+2} \\ g_1^*\sqrt{n+1} & 0 & 0 & g_2\sqrt{n+2} \\ 0 & g_1^*\sqrt{n+2} & g_2^*\sqrt{n+2} & 0 \end{pmatrix}. \tag{7}$$

In the micromaser experiments, the atoms enter the resonator in one of the Rydberg states of the maser transition and emerging atoms are probed for being in one of these two states. If at an initial time t, the atoms are in their upper level, then we find the probability amplitudes at the later time $t+\tau$ as [18]

$$\begin{aligned} C_{aan}(t+\tau) &= A_n^{(1)}(\tau)C_{aan}(t), \\ C_{abn}(t+\tau) &= A_{n-1}^{(2)}(\tau)C_{aan-1}(t), \\ C_{ban}(t+\tau) &= A_{n-1}^{(3)}(\tau)C_{aan-1}(t), \\ C_{bbn}(t+\tau) &= A_{n-2}^{(4)}(\tau)C_{aan-2}(t), \end{aligned} \tag{8}$$

with

$$
\begin{aligned}
A_n^{(1)} &= \frac{\beta' - (g_1^2+g_2^2)}{2\beta'}\cos(\lambda_1\tau) + \frac{\beta' + (g_1^2+g_2^2)}{2\beta'}\cos(\lambda_3\tau),\\
A_n^{(2)} &= \frac{-ig_2^*\sqrt{n+1}}{2\beta'}\left(\frac{\alpha_1'+\beta'}{\lambda_1}\sin(\lambda_1\tau) - \frac{\alpha_1'-\beta'}{\lambda_3}\sin(\lambda_3\tau)\right),\\
A_n^{(3)} &= \frac{-ig_1^*\sqrt{n+1}}{2\beta'}\left(\frac{(\alpha_2'+\beta'}{\lambda_1}\sin(\lambda_1\tau) - \frac{\alpha_2'-\beta'}{\lambda_3}\sin(\lambda_3\tau)\right),\\
A_n^{(4)} &= \frac{2g_1^*g_2^*\sqrt{(n+1)(n+2)}}{\beta'}\left(\cos(\lambda_1\tau) - \cos(\lambda_3\tau)\right), \qquad (9)
\end{aligned}
$$

where $\alpha'_{1(2)} = (4n+7)g_{1(2)}^2 - g_{2(1)}^2$, $\beta' = \{(g_1^2+g_2^2)^2 + 16g_1^2g_2^2(n+1)(n+2)\}^{1/2}$, and

$$
\begin{aligned}
\lambda_{1,3} &= \frac{1}{\sqrt{2}}\{(g_1^2+g_2^2)(2n+3)\\
&\pm \left((g_1^2+g_2^2)^2(2n+3)^2 - 4(n+1)(n+2)(g_1^2-g_2^2)^2\right)^{1/2}\}^{1/2}. \qquad (10)
\end{aligned}
$$

Let us compose the master equation for the micromaser which is modified by two–atomic events. On the basis of the density matrix elements we have the expression as

$$
\begin{aligned}
\rho_{n,n'}(t+\tau) &= C_{aan}(t+\tau)C^*_{aan'}(t+\tau) + C_{abn}(t+\tau)C^*_{abn'}(t+\tau)\\
&+ C_{ban}(t+\tau)C^*_{ban'}(t+\tau) + C_{bbn}(t+\tau)C^*_{bbn'}(t+\tau) \qquad (11)
\end{aligned}
$$

and at the initial time it is expressed as $\rho_{n,n'}(t) = C_{aan}(t)C^*_{aan'}(t)$. In order to obtain the equation of motion for the reduced density matrix of the maser field, we consider the coarse–grained derivative as [20]

$$
\left(\frac{d\rho_{n,n'}}{dt}\right)_{gain} = r_a\left[\rho_{n,n'}(t+\tau) - \rho_{n,n'}(t)\right], \qquad (12)
$$

where r_a is the rate of injection. This term describes the change in $\rho_{n,n'}(t)$ due to a pair of atoms interacting with the field for a time τ. The damping term is given by [20]

$$
\begin{aligned}
\left(\hat{\mathcal{L}}\hat{\rho}\right)_{n,n'} &=\\
&- \frac{\gamma}{2}(\bar{n}_{th}+1)(n+n')\rho_{n,n'}(t) + \gamma(\bar{n}_{th}+1)\sqrt{(n+1)(n'+1)}\rho_{n+1,n'+1}(t)\\
&- \frac{\gamma}{2}\bar{n}_{th}(n+n'+2)\rho_{n,n'}(t) + \gamma\bar{n}_{th}\sqrt{nn'}\rho_{n-1,n'-1}(t); \qquad (13)
\end{aligned}
$$

here $\bar{n}_{th}$ is an average thermal photon number inside the cavity and γ is the cavity decay. The equation of motion can be written in the following form

$$
\frac{d\rho_{n,n'}}{dt} = \left(\frac{d\rho_{n,n'}}{dt}\right)_{gain} + \left(\hat{\mathcal{L}}\hat{\rho}\right)_{n,n'}. \qquad (14)
$$

Substituting the expression (8) into (11) and using (12) and (13), the equation of motion becomes

$$
\begin{aligned}
\dot{\rho}_{n,n'} &= a_{n,n'}\rho_{n,n'}(t) + c_{n-1,n'-1}\rho_{n-1,n'-1}(t)\\
&+ d_{n+1,n'+1}\rho_{n+1,n'+1}(t) + e_{n-2,n'-2}\rho_{n-2,n'-2}(t), \qquad (15)
\end{aligned}
$$

where the dot on the symbol denotes the derivative and the coefficients read

$$\begin{aligned} a_{n,n'} &= -r_a\left(1 - A_n^{(1)}(A_{n'}^{(1)})^*\right) - \gamma\left(\bar{n}_{th}(n+n'+1) + \frac{n+n'}{2}\right), \\ c_{n,n'} &= r_a\left(A_n^{(2)}(A_{n'}^{(2)})^* + A_n^{(3)}(A_{n'}^{(3)})^*\right) + \gamma\bar{n}_{th}\sqrt{(n+1)(n'+1)}, \\ d_{n,n'} &= \gamma(\bar{n}_{th}+1)\sqrt{nn'}, \quad e_{n,n'} = r_a A_n^{(4)}(A_{n'}^{(4)})^*. \end{aligned}$$

It is clear that for $n = n'$ Eq. (15) determines the probability of finding n photons in the cavity in the time $t + \tau$,

$$\begin{aligned} \dot{P}_n(t) = \dot{\rho}_{n,n} &= a_{n,n}P_n(t) + c_{n-1,n-1}P_{n-1}(t) \\ &+ d_{n+1,n+1}P_{n+1}(t) + e_{n-2,n-2}P_{n-2}(t), \end{aligned} \tag{16}$$

where the coefficients read

$$\begin{aligned} a_{n,n} &= -r_a(1 - |A_n^{(1)}|^2) - \gamma(\bar{n}_{th}(2n+1) + n), \\ c_{n,n} &= r_a(|A_{n+1}^{(2)}|^2 + |A_{n+1}^{(3)}|^2) + \gamma\bar{n}_{th}(n+1), \\ d_{n,n} &= \gamma(\bar{n}_{th}+1)n, \quad e_{n,n} = r_a|A_n^{(4)}|^2. \end{aligned}$$

As is seen from (16), besides the coefficients $a_{n,n}$, $c_{n,n}$ and $d_{n,n}$ associated with the usual one–photon transition probabilities, the presence of the second atom leads to a new coefficient $e_{n,n}$ associated with two–photon transitions. One can see from the expression that $e_{n,n} \sim \Delta^2 \ll 1$, as is expected. It may also be noted that [18, 20]

$$a_{n,n} + c_{n,n} + d_{n,n} + e_{n,n} = 0. \tag{17}$$

2.1 Steady–state solutions

Now we deal with the steady–state problem of (16). As is mentioned before, the influence of the two–atomic events is rare, therefore it is physical to consider a steady–state solution in which the 'flows' of the energy in and out the cavity compensate. The steady–state photon number distribution can be obtained from (16) by taking

$$\dot{P}(n) = 0. \tag{18}$$

We can express the steady–state solution as a product of continued fractions [18], so that

$$P(n) = P(0)\prod_{k=1}^{n} Q_k, \tag{19}$$

where

$$Q_k = \frac{1}{d_{k,k}}\left[\begin{array}{c} \alpha_{k-1} + \dfrac{\beta_{k-1}}{\alpha_{k-2} + \dfrac{\beta_{k-2}}{\alpha_{k-3} + \dfrac{\beta_{k-3}}{\vdots \\ \dfrac{}{\alpha_1 + \frac{\beta_1}{\alpha_0}}}}} \end{array}\right], \tag{20}$$

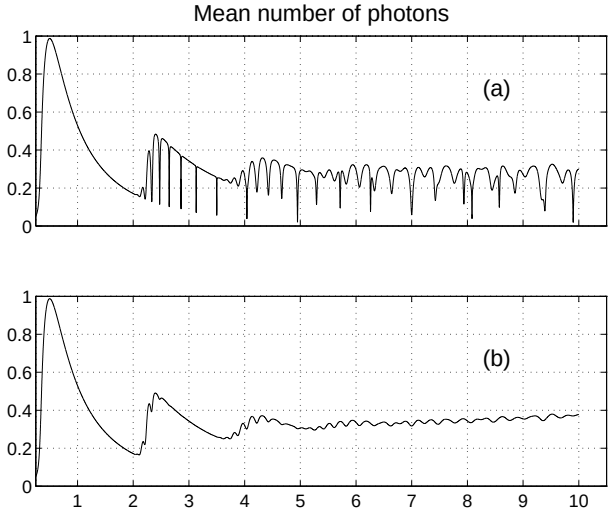

Fig. 1. Normalized mean photon number $l \equiv \langle n \rangle / N_{ex}$ versus the pump parameter θ for $N_{ex} = 49$, $\bar{n}_{th} = 10^{-7}$, $\Delta = 0$ (a) and $\Delta = 0.01$ (b).

with $\alpha_k = c_{k,k} + e_{k,k}$ and $\beta_k = d_{k,k} e_{k-1,k-1}$. This expression for $P(n)$ completely determines the photon statistics caused by co–operative atomic effects in the cavity. Figure 1a shows the normalized average number of photons $l \equiv \langle n \rangle / N_{ex}$, where $N_{ex} \equiv r_a/\gamma$ is the average number of atoms that traverse the cavity during the lifetime of the field as functions of the dimensionless parameter θ defined as [5]

$$\theta = (N_{ex})^{1/2} g_1 \tau \tag{21}$$

for $N_{ex} = 49$. As has been mentioned by Meystre [21] for very–low temperatures (with average thermal photon number $\bar{n}_{th} = 10^{-7}$), the steady–state photon statistics of the micromaser are strongly influenced by the existence of trapping states. (Note that for higher resolution the dips become more distinct.) In contrast, from Fig. 1b, one can see that these peculiar features of the one–atom maser are almost removed by a little amount $\Delta = 0.01$ of co–operative effects involved in. Nevertheless, for a not very high atomic pump rate, $N_{ex} = 25$, the 'hallmarks' of the existence of trapping states, i.e., the dips in Fig. 2a, are still remaining their features when $\Delta = 0.01$ (see Fig. 2b). In general, we could say that the presence of two–atomic events in the cavity disturbs the trapping state condition and an atom can emit a photon.

2.2 Time–dependent approximate solutions

Furthermore, a modified Scully–Lamb master equation (15) can be written in a detailed balance form as [20]

$$\begin{aligned} \dot{\rho}_n^{(k)}(t) &= X_n^{(k)} \rho_n^{(k)}(t) + c_{n-1}^{(k)} \rho_{n-1}^{(k)}(t) - d_n^{(k)} \rho_n^{(k)}(t) \\ &- c_n^{(k)} \rho_n^{(k)}(t) + d_{n+1}^{(k)} \rho_{n+1}^{(k)}(t) + e_{n-2}^{(k)} \rho_{n-2}^{(k)}(t) - e_n^{(k)} \rho_n^{(k)}(t), \end{aligned} \tag{22}$$

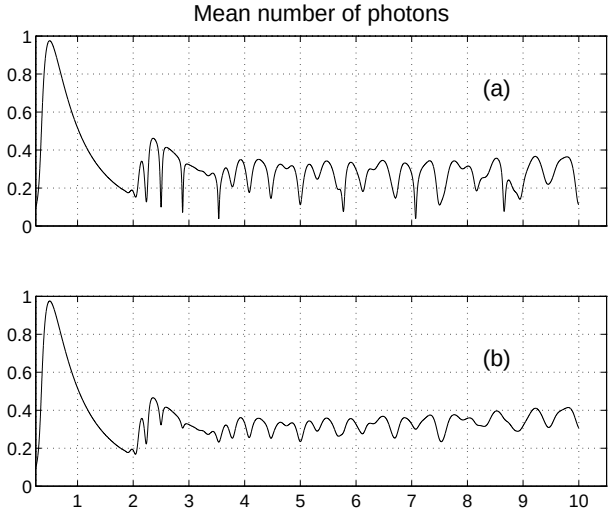

Fig. 2. The same as in Fig. 1, but $N_{ex} = 25$.

where we substitute $n' = n + k$, rewrite $\rho_{n,n'}(t) = \rho_n^{(k)}(t)$, $a_{n,n'} = a_n^{(k)}$, $c_{n,n'} = c_n^{(k)}$, $d_{n,n'} = d_n^{(k)}$, $e_{n,n'} = e_n^{(k)}$ and

$$X_n^{(k)} = a_n^{(k)} + c_n^{(k)} + d_n^{(k)} + e_n^{(k)}. \tag{23}$$

This type of detailed balance master equation was used in [20] in the one–atom maser theory. In that case, the coefficients $e_n^{(k)}$ and $e_{n-2}^{(k)}$ do not appear. Using the fact that $a_0^{(k)} = c_{-1}^{(k)} = d_0^{(k)} = e_{-1}^{(k)} = e_{-2}^{(k)} = 0$, the sum over n in Eq. (22) simply becomes

$$\sum_{n=0}^{\infty} \dot{\rho}_n^{(k)}(t) = \sum_{n=0}^{\infty} \left(X_n^{(k)} \rho_n^{(k)}(t) \right), \tag{24}$$

which has as a solution

$$\rho_n^{(k)}(t) = \rho_n^{(k)}(0) \exp(X_n^{(k)} t). \tag{25}$$

Note that if the density matrix is initially diagonal, then it remains diagonal for all time.

3 Calculations of the spectrum

We now turn to the calculation of the micromaser spectrum which is originated from the simple Hamiltonian (1) including pair–atomic effects. Although the spectrum of the micromaser cavity field is not directly detected, it can include many of interesting features. The micromaser spectrum is given as the Fourier transform

$$S(\omega - \omega_c) = \mathrm{Re} \int_0^{\infty} K(t) \mathrm{e}^{-i(\omega - \omega_c)t} dt \tag{26}$$

of the two–time correlation function

$$K(t) = \langle \hat{a}^{\dagger}(t)\hat{a}(0)\rangle, \tag{27}$$

which is related to the time dependence of the off-diagonal elements of the field density matrix. Here ω_c denotes the frequency of the cavity field. The central problem of the calculation of the micromaser spectrum is therefore to find the time dependence of $K(t)$. In the next stage, we consider two different but equivalent methods calculating the linewidth of the micromaser.

3.1 Exact numerical method: Eigenvalue approach

We mainly follow the work by Vogel et al. [11] and investigate how atomic co–operative effect does modify the exact spectrum of the one–atom maser. The two–time correlation function can read

$$K(t) = \mathrm{Tr}_{f,r}\left[\hat{U}^{\dagger}(t)\hat{a}^{\dagger}(0)\hat{U}(t)\hat{a}(0)\hat{\rho}_{f,r}(0)\right], \tag{28}$$

thus,

$$K(t) = \mathrm{Tr}_{f}\left[\hat{a}^{\dagger}(0)\hat{\tilde{\rho}}(t)\right] \tag{29}$$

with

$$\hat{\tilde{\rho}}(t) = \mathrm{Tr}_{r}\left[\hat{U}(t)\hat{a}(0)\hat{\rho}_{f,r}(0)\hat{U}^{\dagger}(t)\right], \tag{30}$$

where the time evolution operator of the combined field (f)–reservoir (r) system is used. In the Markov approximation the operator $\hat{\tilde{\rho}}(t)$ satisfies the same equation of motion for the field density operator $\hat{\rho}$, but with the initial condition

$$\hat{\tilde{\rho}}(0) = \hat{a}(0)\hat{\rho}(0), \tag{31}$$

and, consequently, we can choose the steady–state solution of the field density operator $\hat{\rho}^{(s)}$ as the initial condition, that is,

$$\tilde{\rho}_{n,n+1}(0) = \sqrt{n+1}P_{n+1}, \tag{32}$$

where the steady–state photon statistics $P(n)$ are given by (19). In the next stage, after performing the trace in (29), we find

$$K(t) = \sum_{n=0}^{\infty}\sqrt{n+1}\tilde{\rho}_{n,n+1}(t). \tag{33}$$

As in [11], one can interpret the matrix elements $\tilde{\rho}_n^{(k)}$(t) as the nth component of the vector $\mathbf{x}^k(t)$, i.e.,

$$\left(\mathbf{x}^{(k)}(t)\right)_n \equiv \tilde{\rho}_n^{(k)}(t). \tag{34}$$

Recalling that $\tilde{\rho}_n^{(k)}(t)$ satisfies (15) with $\tilde{\rho}_n^{(k)}(t)$ replacing $\rho_n^{(k)}(t)$, the equation of motion for the vector $\mathbf{x}^{(k)}(t)$ becomes

$$\dot{\mathbf{x}}^{(k)} = \mathbf{Q}^{(k)}\mathbf{x}^{(k)}, \tag{35}$$

where the matrix $\mathbf{Q}^{(k)}$ is composed of four diagonals, while in the one–atom maser theory, it is composed of three diagonals, with the elements

$$Q^{(k)}_{n,n} = a^{(k)}_n,\ Q^{(k)}_{n,n+1} = d^{(k)}_{n+1},\ Q^{(k)}_{n,n-1} = c^{(k)}_{n-1},\ Q^{(k)}_{n,n-2} = e^{(k)}_{n-2}. \tag{36}$$

Since only $\mathbf{x}^{(1)}(t)$ be needed to determine $K(t)$ according to (33), the time–dependent solution of (35) (for $k = 1$) can be found

$$\mathbf{x}^{(1)}(t) = \sum_l B^{(1)}_l \mathbf{x}^{(1)}(0) A^{(1)}_l \mathrm{e}^{-\lambda^{(1)}_l t}, \tag{37}$$

with the initial condition $\left[\mathbf{x}^{(1)}(0)\right]_n \equiv \tilde{\rho}^{(1)}_n(0)$, and we have to calculate the eigenvalues $\lambda^{(1)}_l$ as well as the right– and left–sided eigenvectors $A^{(1)}_l$ and $B^{(1)}_l$ of the matrix $\mathbf{Q}^{(1)}$, respectively. The Fourier transform of (33)

$$S(\omega - \omega_c) = \mathrm{Re} \sum_{l=0}^{\infty} \frac{K_l}{\lambda^{(1)}_l + i(\omega - \omega_c)}, \tag{38}$$

is then the spectrum of the micromaser, where

$$\begin{aligned} K_l &= \sum_{n=0}^{\infty} \sqrt{n+1} \sum_{m=0}^{\infty} \left(A^{(1)}_l\right)_n \left(B^{(1)}_l\right)_m \tilde{\rho}^{(1)}_m(0) \\ &= \left[\sum_{n=0}^{\infty} \sqrt{n+1} \left(A^{(1)}_l\right)_n\right] \times \left[\sum_{m=0}^{\infty} \sqrt{m+1} \left(B^{(1)}_l\right)_m P_{m+1}\right]. \end{aligned} \tag{39}$$

It consists of Lorentzian distributions, weighted by K_l. The full width at half maximum (FWHM) of each individual Lorentzian distribution is the real part of the eigenvalue $2\lambda^{(1)}_l$.

3.2 Approximate analytical solution: Green–function approach

We first express the correlation function (27) with the help of the Green–function of the master equation for the field density operator following the work by Tran–Quang et al. [9]. We can rewrite (28) as

$$\begin{aligned} K(t) &= \mathrm{Tr}_{f,r}\left[\hat{a}^\dagger(0)\hat{U}(t)\hat{a}(0)\hat{\rho}_{f,r}(0)\hat{U}^\dagger(t)\right] \\ &= \sum_{l,m} G^{(m)}_{l,l+1}(t)\sqrt{(l+1)(m+1)}P_{m+1}, \end{aligned} \tag{40}$$

where the Green function $G^{(m)}_{l,l+1}(t)$ with the initial condition $G_{l,l+1}(0) = \delta_{l,m}$ is a matrix element of the operator

$$\hat{G}^{(m)}(t) = \mathrm{Tr}_r\left[\hat{U}(t)|m\rangle\langle m+1|\hat{\rho}^{(s)}_r\hat{U}^\dagger(t)\right], \tag{41}$$

with $U_{j,k} = \langle j|\hat{U}(t)|k\rangle$ and $U^\dagger_{j,k} = \langle j|\hat{U}^\dagger(t)|k\rangle$. To obtain (40), we have assumed that at the steady state, that is at time $t = 0$, the density operator $\hat{\rho}_{f,r}(0)$ can be factorized into that of

the field $\hat{\rho}^{(s)}$ and the reservoir $\hat{\rho}_r^{(s)}$ and the steady–state field density matrix is diagonal. Note that the operator $\hat{G}^{(m)}(t)$ must obey the same master equation as the field density operator $\hat{\rho}(t)$. Therefore, it is clear from the obtained solution (25) that the element of the Green–function does take the solution

$$G_{l,l+1}^{(m)}(t) = \delta_{n,m} \mathrm{e}^{X_l^{(1)} t}, \tag{42}$$

where $X_n^{(1)}$ is given by (23). Substituting this solution into (40), we obtain

$$K(t) = \sum_m (m+1) P_{m+1} \mathrm{e}^{X_n^{(1)} t}. \tag{43}$$

The unnormalized spectrum (26) immediately becomes

$$S(\omega - \omega_c) = \sum_{n=0}^{\infty} \frac{(n+1) P_{n+1} \left| X_n^{(1)} \right|}{\left(X_n^{(1)} \right)^2 + (\omega - \omega_c)^2} \tag{44}$$

using the fact that $X_n^{(1)} < 0$. This is a sum (on n) of Lorentzians, each with linewidth $2 \left| X_n^{(1)} \right|$.

4 Discussion of the results

Now we demonstrate that the approximate spectrum matches the exact one much more accurately. To do this, we solve the equation with respect to $\Delta\omega$

$$I(\nu + \Delta\omega) = \frac{1}{2} I(\nu) \tag{45}$$

(where ν is the micromaser frequency) for the spectrum (44), in order to find the approximate FWHM $2\Delta\omega_{ap}$. We also apply such a search routine to the exact spectrum (38), to determine the exact $2\Delta\omega_{ex}$. We show in Fig. 3 the approximate linewidth along with the exact linewidth for $N_{ex} = 50$, $\bar{n}_{th} = 0.0001$ and $\Delta = 0$ in range of the pumping parameter θ. The dotted curve represents the approximation while the solid curve represents $2\Delta\omega_{ex}$. In Fig. 4, the approximate and the exact linewidths are depicted in the case of non–zero Δ. We see that even for this case, the two spectra are close each other. As is seen from Fig. 5, the little narrowing of the natural linewidth is obtained when the one atomic behaviour in the micromaser is influenced by the pair–atomic events.

In conclusion, we have dealt with the modification of the micromaser theory, from the view point of the presence of co–operative atomic events. A standard Jaynes–Cummings Hamiltonian has been modified by the effect of the pair of atoms. The probability amplitude method has been adopted to find the solution of the equation of motion, which is the modified Scully–Lamb master equation derived for the field density matrix elements. We have found the expression for the coefficients associated with the probability for two–photon transitions in the micromaser cavity. The steady–state solution has been found showing that the trapping states can disappear by the small influence caused by atomic co–operative effects. Based on the approximate and exact solution of the master equations, we have calculated the micromaser spectrum which gives rise to the narrower linewidth compared to that obtained in the one–atom maser theory.

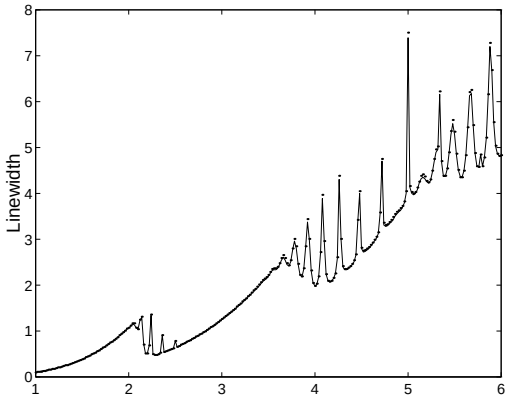

Fig. 3. Comparison of linewidths FWHM/γ of the approximate (the dotted curve) and the exact spectrum (the solid curve) as functions of the pump parameter θ, where $N_{ex} = 50,\ \bar{n}_{th} = 0.0001,\ \Delta = 0$.

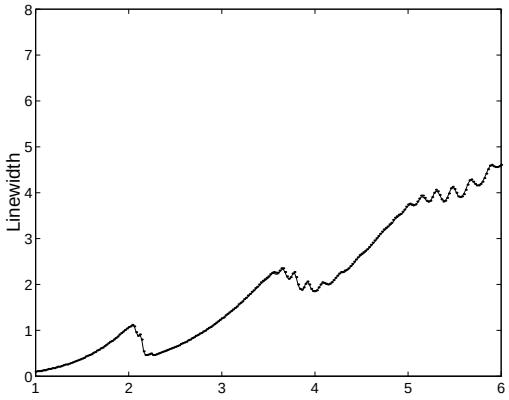

Fig. 4. Comparison of linewidths FWHM/γ of the approximate (the dotted curve) and the exact spectrum (the solid curve) as functions of the pump parameter θ, where $N_{ex} = 50,\ \bar{n}_{th} = 0.0001,\ \Delta = 0.01$.

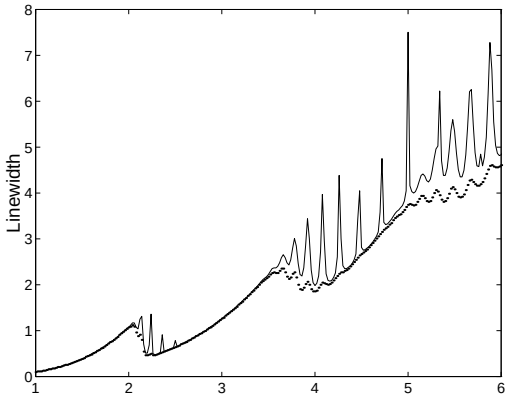

Fig. 5. Comparison of linewidths FWHM/γ calculated by the one–atom maser theory (the solid curve) (as in Fig. 3) and the presented theory with including co–operative effects (dotted curve) (as in Fig. 4).

Acknowledgments This work was supported by Complex Grant No VS96028 and Research Project CEZ: J14/98 of the Czech Ministry of Education, and by Grant No 202/00/0142 of Czech Grant Agency.

References

[1] D. Meschede, H. Walther, G. Müller: *Phys. Rev. Lett.* **54** (1985) 551

[2] M. Weidinger, B.T.H. Varcoe, R. Heerlein, H. Walther: *Phys. Rev. Lett.* **82** (1999) 3795

[3] G. Rempe, H. Walther, N. Klein: *Phys. Rev. Lett.* **58** (1987) 353

[4] J. Peřina: *Quantum Statistics of Linear and Nonlinear Optical Phenomena*, 2nd edition, Kluwer, Dordrecht, 1991

[5] J. Filipowicz, J. Javanainen, P. Meystre: *Phys. Rev. A* **34** (1986) 3077; L.A. Lugiato, M.O. Scully, H. Walther: *ibid.* **36** (1987) 740; G. Rempe, H. Walther: *ibid.* **42** (1990) 1650

[6] J. Krause, M.O. Scully, H. Walther: *Phys. Rev. A* **36** (1987) 4547; J. Krause, M.O. Scully, T. Walther, H. Walther: *ibid.* **39** (1989) 1915

[7] F.L. Kien: *Phys. Rev. A* **44** (1991) 3282; J.J. Slosser, P. Meystre: *ibid.* **41** (1990) 3867; F.L. Kien, M.O. Scully, H. Walther: *Found. Phys.* **23** (1993) 177; G. Ariunbold, J. Peřina, Ts. Gantsog: *Quantum Semiclass. Opt.* **1** (1999) 219

[8] J. Krause, M.O. Scully, H. Walther: *Phys. Rev. A* **34** (1986) 2032; R.R. McGowan, W.C. Schieve: *ibid.* **56** (1997) 2373

[9] T. Quang, G.S. Agarwal, J. Bergou, M.O. Scully, H. Walther: *Phys. Rev. A* **48** (1993) 803

[10] N. Lu: *Phys. Rev. A* **47** (1993) 1347; N. Lu: *Opt. Commun.* **103** (1993) 315

[11] K. Vogel, W.P. Schleich, M.O. Scully, H. Walther: *Phys. Rev. A* **48** (1993) 813

[12] R.R. McGowan, W. C. Schieve: *Phys. Rev. A* **55** (1997) 3813

[13] M. Brune, J.M. Raimond, S. Haroche: *Phys. Rev. A* **35** (1987) 154; L. Davidovich, J.M. Raimond, M. Brune, S. Haroche: *ibid.* **36** (1987) 3771; I. Ashraf, J. Gea–Banacloche, M.S. Zubairy: *ibid.* **42** (1990) 6704; I. Ashraf, M.S. Zubairy: *Opt. Commun.* **77** (1990) 85

[14] M. Brune, J.M. Raimond, P. Goy, L. Davidovich, S. Haroche: *Phys. Rev. Lett.* **59** (1987) 1899

[15] A.H. Toor, S.-Y. Zhu, S. Zubairy: *Phys. Rev. A* **53** (1996) 3529

[16] M. Orszag, R. Ramírez, J.C. Retamal, C. Saavedra: *Phys. Rev. A* **49** (1994) 2933

[17] E. Wehner, R. Seno, N. Sterpi, B.-G. Englert, H. Walther: *Opt. Commun.* **110** (1994) 655

[18] S. Mahmood, M.S. Zubairy: *Phys. Rev. A* **35** (1987) 425; I. Ashraf, N. Jehan, M. Majeed: unpublished

[19] G. Yeoman, G. M. Meyer: *Phys. Rev. A* **58** (1998) 2518

[20] M.O. Scully, M.S. Zubairy: *Quantum Optics*, Cambridge University Press, Cambridge, 1997

[21] P. Meystre, G. Rempe, H. Walther: *Opt. Lett. A* **13** (1988) 1078